Supporting Information

Photoactive oligomer with D-D'-A-D'-D''-D'-A-D'-D scaffold for high-efficiency NIR-II phototheranostics

Qi Wang,[a,1] Jiawei Liu,[a,1] Xinmin Zhang,[a] Youguang Tang,[a] Yanwei Xiong,[a] Liangliang Zhang,[b] Tangxin Xiao [b] and Quli Fan*[a]

[a] *State Key Laboratory for Organic Electronics and Information Displays & Institute of Advanced Materials (IAM), Nanjing University of Posts & Telecommunications, Nanjing 210023, China. E-mail: iamqlfan@njupt.edu.cn.*

[b] *Jiangsu Key Laboratory of Advanced Catalytic Materials and Technology, School of Petrochemical Engineering, Changzhou University, Changzhou, 213164, China.*

Table of Contents

1. General information and experimental procedure

General information

All reactions were performed in atmosphere unless noted. The commercially available reagents and solvents were either employed as purchased or dried according to procedures described in the literature. Materials for synthesis O-BT were purchased from Suna Tech Inc. Mice, NIH-3T3 and Hela cells were provided by Jiangsu KeyGEN BioTECH Corp., Ltd. ^{1}H NMR and ^{13}C NMR spectra were tested on a Bruker AVANCE III instrument. The matrix-assisted laser desorption/ionization time-of-flight (MALDI-TOF) mass spectra were measured by a Bruker Autoflex TOF/TOF spectrometer. The morphology and size of NPs were determined by a HT7700 transmission electron microscope (TEM) and a particle size analyzer (Brookhaven Instruments), respectively. Absorption and emission spectra were obtained using a UV3600 UV/vis/NIR spectrophotometer (Shimadzu) and an NIR-II spectrophotometer (Fluorolog 3, Horiba), respectively. The MTT experiments were conducted using a microplate reader (Bio-Rad Laboratories, Hercules). The flow cytometry experiments were conducted through a Flow Sight Imaging Flow Cytometer (Merck Millipore, Darmstadt, Germany).

Experimental procedure

Preparation of O-BT NPs

The solution of O-BT (1mg) and F127 (10mg) in THF (1 mL) was added into water (10 mL), and the mixture was ultrasound emulsification for 2 min. After blow off THF with nitrogen and centrifugation, O-BT NPs solution was obtained.

Photothermal measurement

O-BT NPs solution (a series of concentrations) and water were irradiated with 808 nm laser (1 W/cm^2). IR thermal camera was used to detect the temperature change of

solution. Moreover, the temperature changes of O-BT NPs (100μg/mL) upon 808 nm laser (a series of power densities) irradiation were also detected.

Cell cytotoxicity assay

After incubated Hela cells in culture medium for 24 h, O-BT NPs at varying concentrations were further cultured with cells. Then the cells were treated with 808 nm laser illumination. After further incubation and PBS wash, MTT solution was added into each well for analysis of the cell viabilitiy.

For live/dead cell staining assay: refer to the above for cell culture. After laser irradiation, calcein AM (mark live cells) and propidium iodide (PI, mark dead cells) were used to stain with cells.

For flow cytometry: after laser irradiation, Annexin V-FITC and PI were used to stain with cells.

Live subject statement

All of the experiments in this study were performed in compliance with the guidelines of Jiangsu Administration of Experimental Animals, and the experiments were approved by the Animal Ethics Committee of Simcere BioTech Corp., Ltd.

Animal model

Female Balb/c nude mice were bought from Jiangsu KeyGEN BioTECH Corp. The Hela tumor-bearing mouse model was established by subcutaneous injection of Hela tumor cells (1×10^6 cells) in the right forelimb armpit of nude mice. The mice were used for imaging when the tumor grew to 100 mm^3.

In vivo NIR-II FLI

After tail intravenous injection of O-BT NPs into Hela tumor-bearing mice, NIRvana 640 InGaAs camera was used to real-time detect the NIR-II signals at the tumor site.

2. *Synthesis of O-BT*

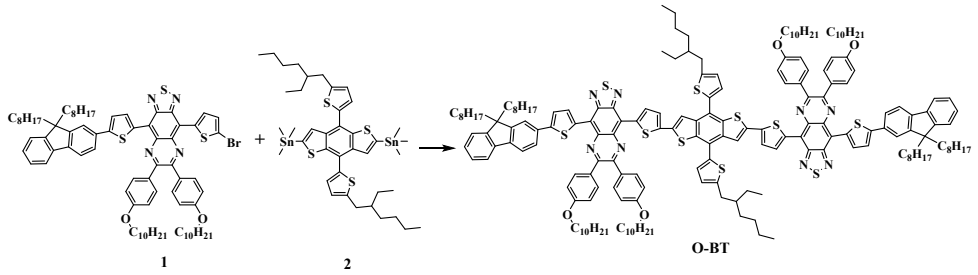

Scheme S1. Synthesis of O-BT.

Under nitrogen atmosphere, compound 1 (50 mg, 0.04 mmol), tetrakis(triphenylphosphine)palladium (2 mg) were put into a two-necked flask, and then compound 2 (18.1 mg, 0.02 mmol) and toluene (10 mL) were injected. The reaction was stirred and refluxed at 100 °C for 24 h under experimental conditions. After the reaction was completed, the reaction solution was cooled to room temperature, and 30 mL of saturated aqueous potassium fluoride solution was added to the reaction flask. Finally, through DCM extraction, rotary evaporation and column chromatography purification, compound O-BT was obtained. ^{1}H NMR (400 MHz, $CDCl_3$, δ) 8.87 (d, 2H), 8.77 (d, 2H), 8.00 (d, 4H), 7.86 (d, 4H), 7.77-7.69 (m, 10H), 7.47 (d, 2H), 7.43-7.36 (m, 6H), 7.34-7.32 (m, 2H), 7.21-7.20 (m, 4H), 7.09 (d, 4H), 7.01 (d, 4H), 4.16-4.09 (m, 8H), 3.08 (d, 4H), 2.15 (br, s, 8H), 1.99-1.85 (m, 10H), 1.49-1.42 (m, 64H), 1.26-1.02 (m, 50H), 0.92-0.75 (m, 42H). MS (MALDI-TOF, m/z) Calcd for $C_{188}H_{230}N_8O_4S_{10}$, 2986.560; Found: 2986.568.

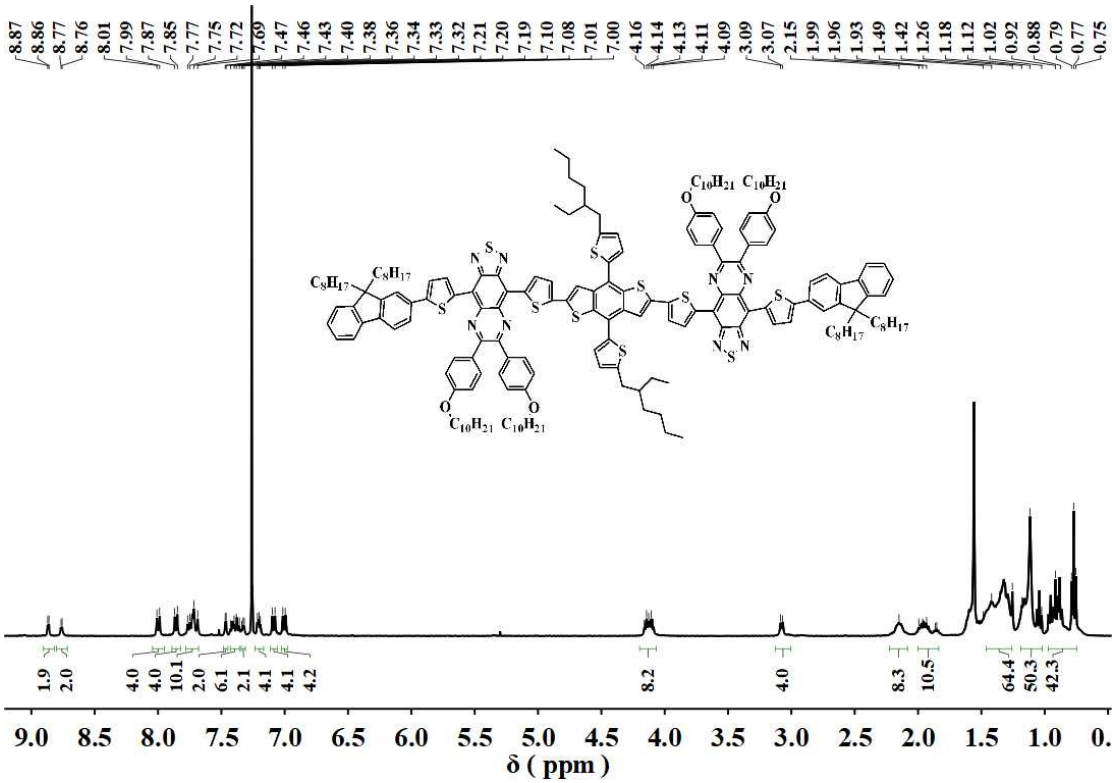

Fig. S1 ^{1}H NMR spectrum of O-BT.

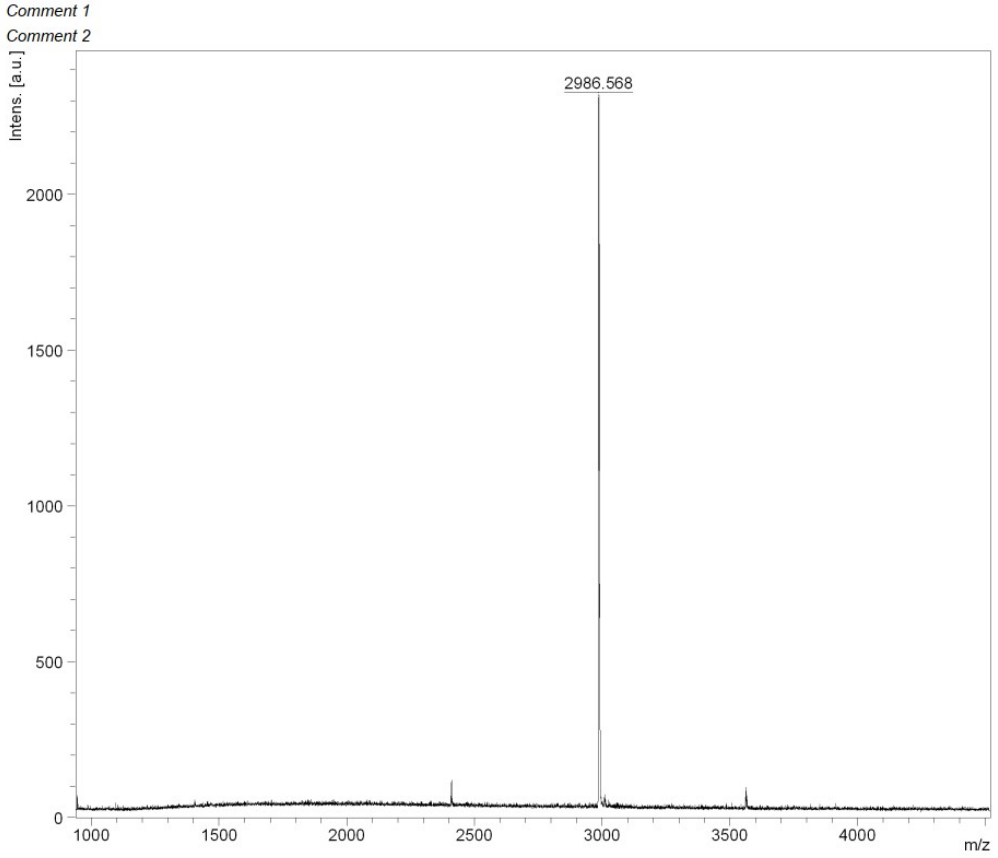

Fig. S2 MOLDI-TOF-MS spectrum of O-BT.

3. *Absorption and fluorescence spectra of O-BT in THF*

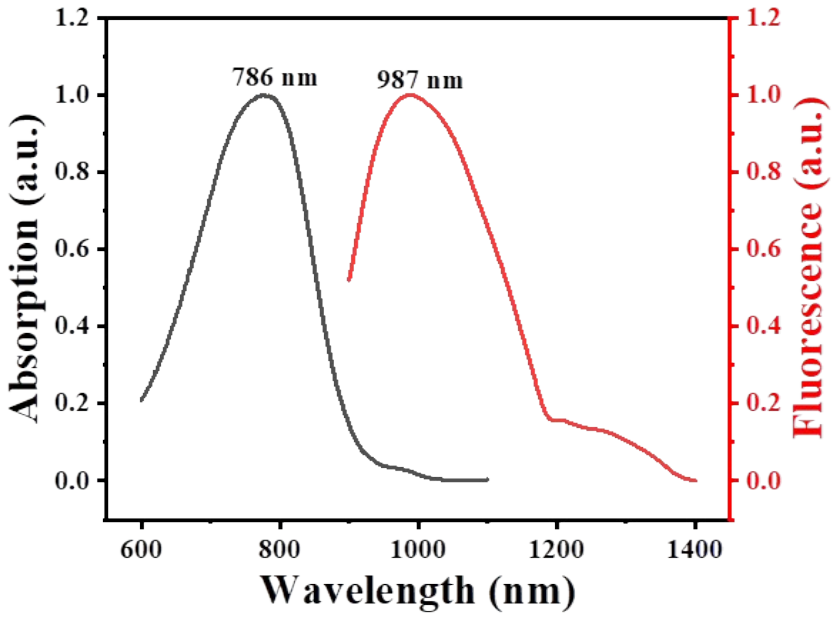

Fig. S3 Absorption and fluorescence spectra of O-BT in THF.

4. *Molar absorption coefficient of O-BT NPs*

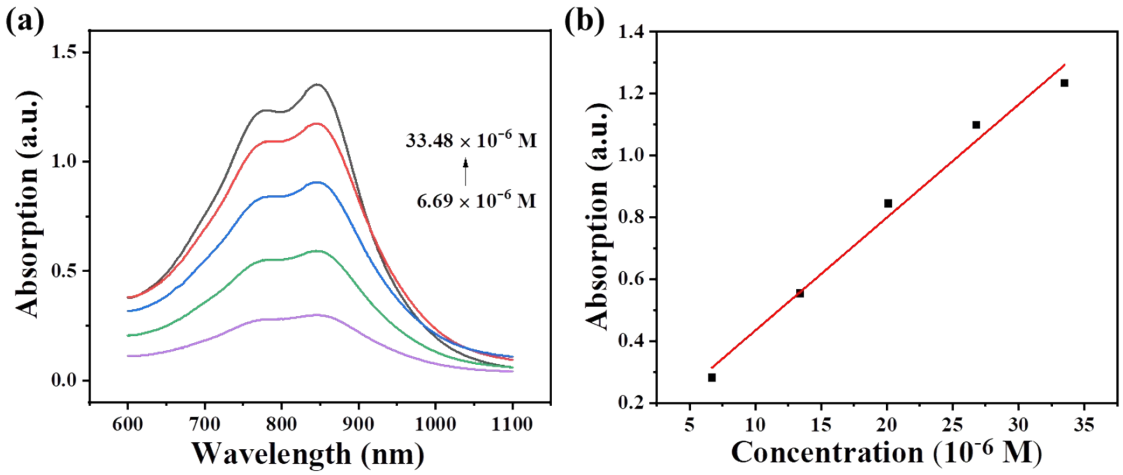

Fig. S4 (a) Absorption curves of O-BT NPs aqueous solution at different concentrations. (b) Linear absorbance versus concentration obtained from (a).

5. *Fluorescence quantum yield measurements of O-BT NPs*

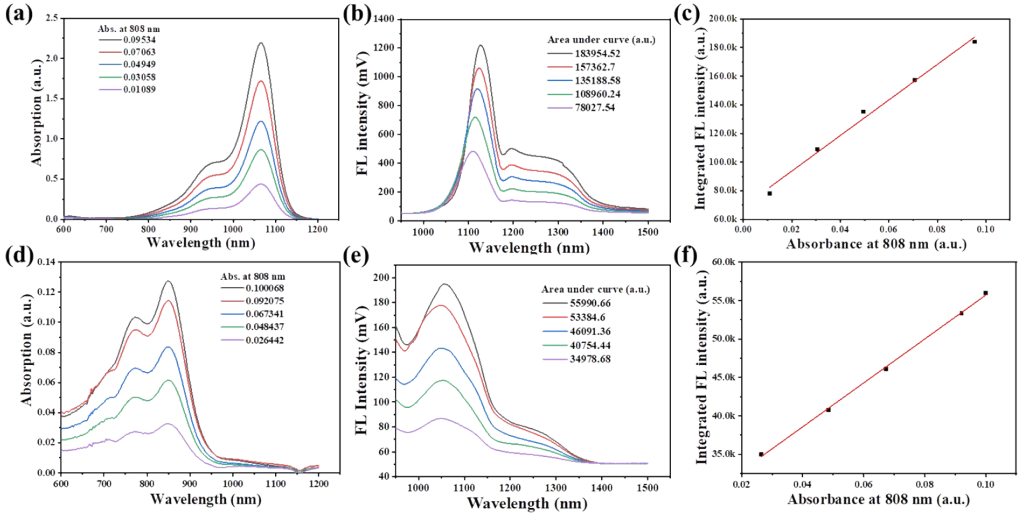

Fig. S5 (a) UV-Vis-NIR spectra of IR-1061 with different concentrations. (b) NIR emission spectra of IR-1061 different concentrations under 808 nm excitation. AUC in the emission spectra for each solution was then calculated and listed in the right of the figure. (c) For all IR-1061solutions, their absorbance values were then plotted versus AUC, and fitted into a linear function. (d) UV-Vis-NIR spectra of O-BT NPs with different concentrations. (e) NIR emission spectra of O-BT NPs different concentrations under 808 nm excitation. AUC in the emission spectra for each solution was then calculated and listed in the right of the figure. (f) For all O-BT NPs solutions, their absorbance values were then plotted versus AUC, and fitted into a linear function.

6. *Cellular uptake of NPs*

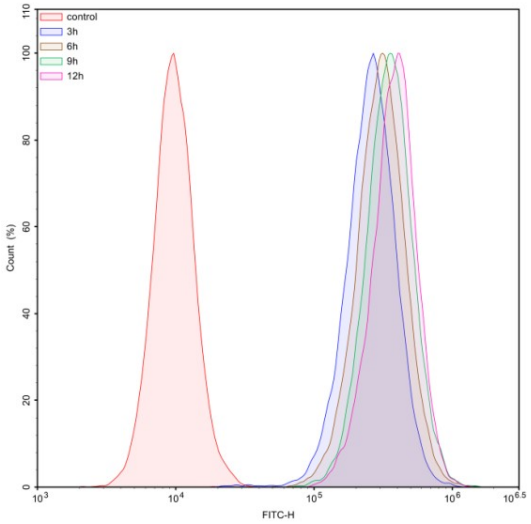

Fig. S6 The cellular uptake of NPs toward Hela cells evaluated by flow cytometry.

7. *The therapeutic efficiency of O-BT NPs appraised by flow cytometry*

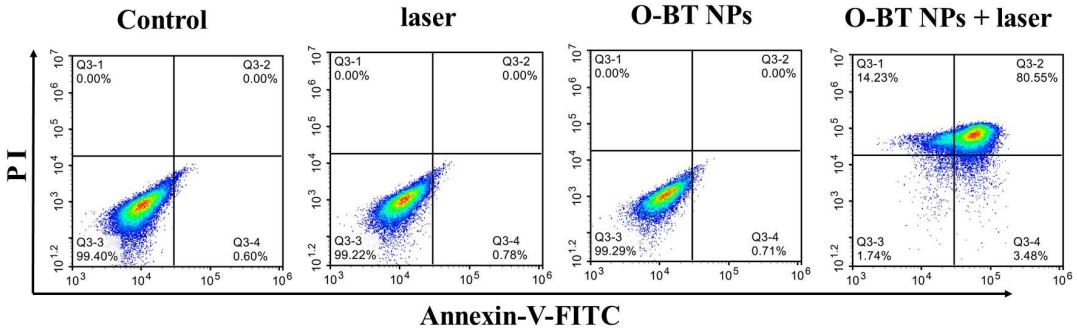

Fig. S7 The therapeutic efficiency of O-BT NPs upon 808 nm laser illumination was further appraised by flow cytometry.

8. *In vitro NIR-II signals of O-BT NPs at different concentrations*

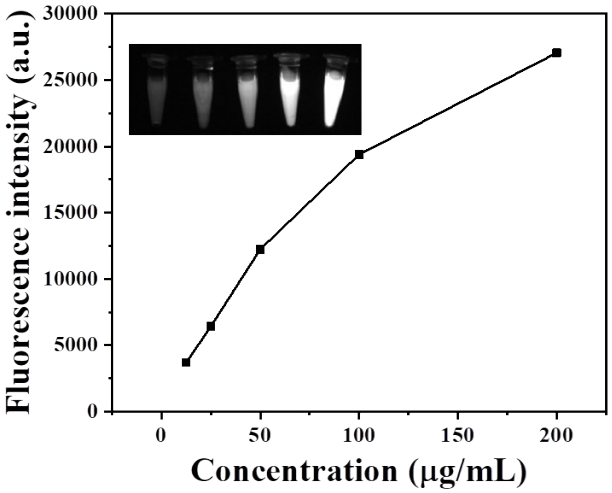

Fig. S8 In vitro NIR-II signals of O-BT NPs at different concentrations

9. *Penetration depth measurement of O-BT NPs*

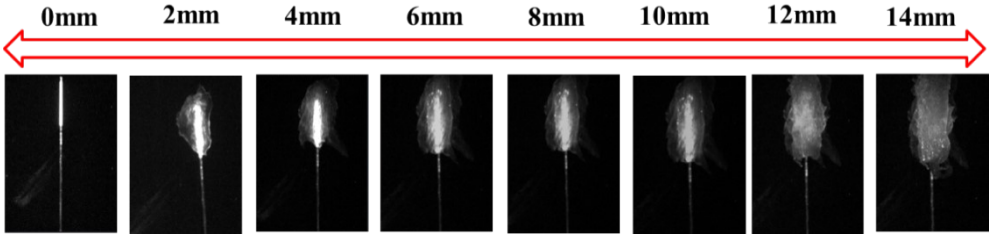

Fig. S9 Penetration depth measurement of O-BT NPs in a simulated deep-tissue setting (chicken tissues).

10. Measurement of FWHM and SBR of vessel 2

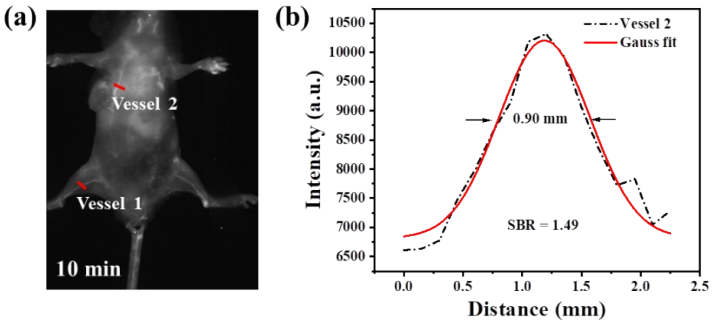

Fig. S10 (a) NIR-II FLI of vessel structures based on O-BT NPs after 10 min injection. (b) Measurement of FWHM and SBR of vessel 2.

11. Ex vivo NIR-II signal intensity of tumor and major organs

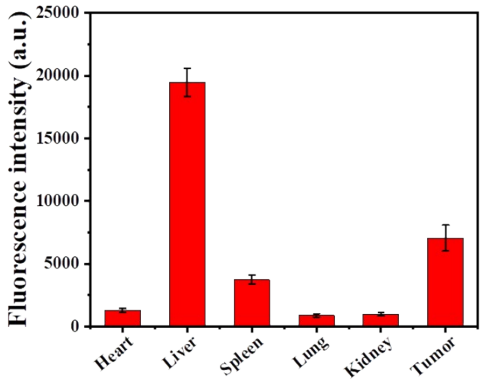

Fig. S11 Ex vivo NIR-II signal intensity of tumor and major organs.

12. Body weight changes of healthy mice treated with PBS and NPs

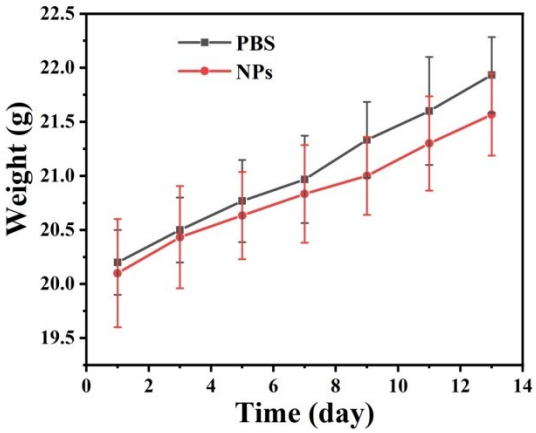

Fig. S12. The body weight changes of healthy mice treated with PBS and NPs within two weeks.